Quark and Meson Spectral Functions with the Functional Renormalization Group

Ralf-Arno Tripolt, ECT*, Trento, Italy

In collaboration with:
Chris Jung, Fabian Rennecke, Naoto Tanji,
Lorenz von Smekal, Jochen Wambach, Johannes Weyrich

Workshop on "Emergent mass and its consequences in the Standard Model"
ECT*, Trento, Italy, September 17-21, 2018

ECT*
EUROPEAN CENTRE FOR THEORETICAL STUDIES
IN NUCLEAR PHYSICS AND RELATED AREAS

CRC-TR 211

Outline

I) Theoretical setup

- Functional Renormalization Group (FRG)
- QCD effective model
- Analytic continuation procedure

II) Results

- Quark spectral function
- (Pseudo-)scalar meson spectral functions
- (Axial-)vector meson spectral functions
- Electromagnetic spectral function and dilepton rates

III) Summary and outlook

I) Theoretical setup

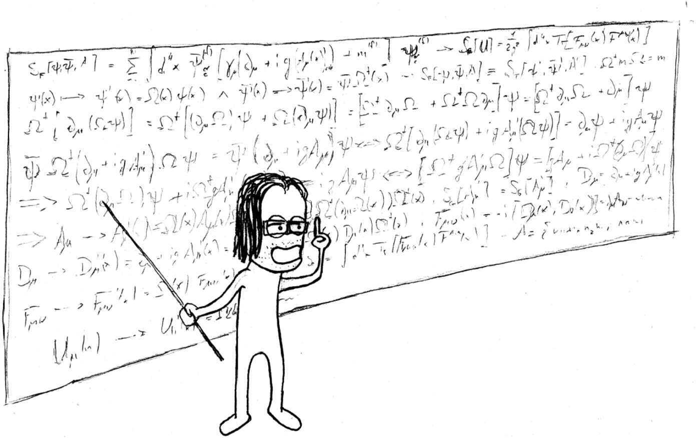

[courtesy L. Holicki]

Consistent theoretical framework

How are in-medium modifications of hadrons related to the change of the vacuum structure of QCD? (deconfinement and chiral symmetry restoration,...)

$\rightarrow$ want a theoretical framework for computing the thermodynamic and the spectral properties of QCD matter on the **same footing!**

Requirements:

- thermodynamic consistency
- preservation of symmetries and their breaking pattern

Candidates:

- mean-field theory
- Functional Renormalization Group (FRG)
- $\cdots$ $\cdots$

FRG includes both **thermal** and **quantum** fluctuations and hence properly deals with phase transitions!

Functional Renormalization Group

Euclidean partition function for a scalar field:

$$Z[J] = \int \mathcal{D}\varphi \ \exp\left(-S[\varphi] + \int d^4x \ J(x)\varphi(x)\right)$$

Wilson's coarse-graining: split φ into low- and high-frequency modes

$$\varphi(x) = \varphi_{q\leq k}(x) + \varphi_{q>k}(x)$$

only include fluctuations with $q > k$

$$Z[J] = \int \mathcal{D}\varphi_{q\leq k} \underbrace{\int \mathcal{D}\varphi_{q>k} \ \exp\left(-S[\varphi] + \int d^4x J(x)\varphi(x)\right)}_{Z_k[J]}$$

Functional Renormalization Group

Scale-dependent partition function can be defined as

$$Z_k[J] = \int \mathcal{D}\varphi \, \exp\left(-S[\varphi] - \Delta S_k[\varphi] + \int d^4x J(x)\varphi(x)\right)$$

by introducing a regulator term that suppresses IR modes

$$\Delta S_k[\varphi] = \frac{1}{2} \int \frac{d^4q}{(2\pi)^4} \, \varphi(-q) R_k(q) \varphi(q)$$

Switch to scale-dependent effective action ($\phi(x) = \langle \varphi(x) \rangle$):

$$\Gamma_k[\phi] = \sup_J \left(\int d^4x \, J(x)\phi(x) - \log Z_k[J] \right) - \Delta S_k[\phi]$$

Functional Renormalization Group

Flow equation for the effective average action Γ_k:

$$\partial_k \Gamma_k = \frac{1}{2}\mathrm{STr}\left(\partial_k R_k \left[\Gamma_k^{(2)} + R_k\right]^{-1}\right)$$

[C. Wetterich, Phys. Lett. **B 301** (1993) 90]

$$\partial_k \Gamma_k \;=\; \frac{1}{2}$$ 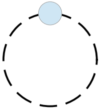

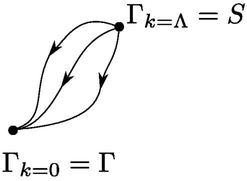

[wikipedia.org/wiki/Functional_renormalization_group]

- Γ_k interpolates between bare action S at $k = \Lambda$ and effective action Γ at $k = 0$
- regulator R_k acts as a mass term and suppresses fluctuations with momenta smaller than k
- the use of 3D regulators allows for a simple analytic continuation procedure

Quark-meson model

Ansatz for the scale-dependent effective average action:

$$\Gamma_k[\overline{\psi}, \psi, \phi] = \int d^4x \left\{ \overline{\psi} \left(\not{\partial} + h(\sigma + i\vec{\tau}\vec{\pi}\gamma_5) - \mu\gamma_0 \right) \psi + \frac{1}{2}(\partial_\mu \phi)^2 + U_k(\phi^2) - c\sigma \right\}$$

- effective low-energy model for QCD with two flavors
- describes spontaneous and explicit chiral symmetry breaking
- flow equation for the effective average action:

$$\partial_k \Gamma_k = \frac{1}{2}$$

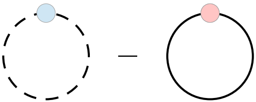

Flow of the effective potential at $\mu = 0$ and $T = 0$

(Loading movie...)

Flow equations for two-point functions

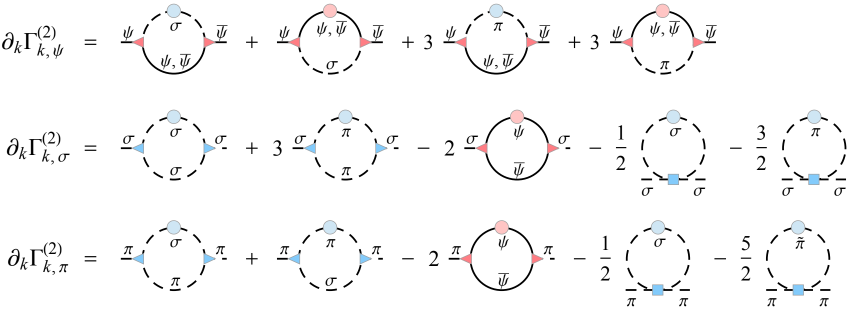

- quark-meson vertices are given by $\Gamma^{(3)}_{\bar{\psi}\psi\sigma} = h$, $\Gamma^{(3)}_{\bar{\psi}\psi\vec{\pi}} = ih\gamma^5\vec{\tau}$
- mesonic vertices from scale-dependent effective potential: $U^{(3)}_{k,\phi_i\phi_j\phi_m}$, $U^{(4)}_{k,\phi_i\phi_j\phi_m\phi_n}$
- one-loop structure and 3D regulators allow for a simple analytic continuation!

[R.-A. Tripolt, L. von Smekal, and J. Wambach, Phys. Rev. **D 90**, 074031 (2014)]

The analytic continuation problem

Calculations at finite temperature are often performed using imaginary energies:

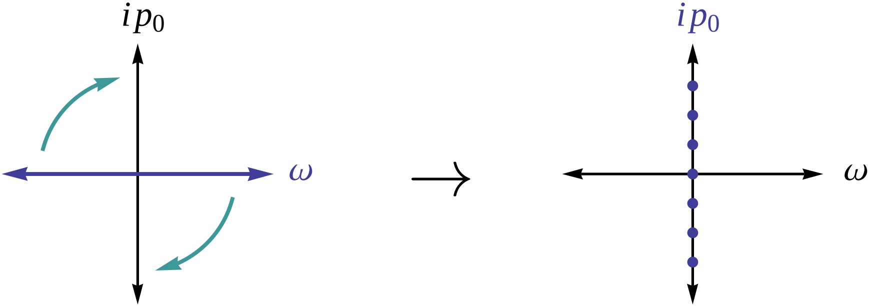

The analytic continuation problem

Analytic continuation problem: How to get back to real energies?

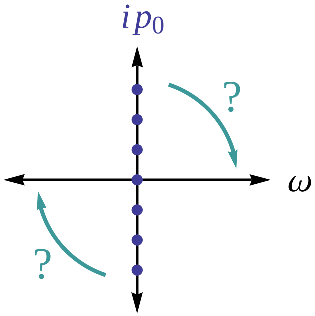

Two-step analytic continuation procedure

1) Use periodicity w.r.t. imaginary energy $ip_0 = i2n\pi T$:

$$n_{B,F}(E + ip_0) \to n_{B,F}(E)$$

2) Substitute p_0 by continuous real frequency ω:

$$\Gamma^{(2),R}(\omega, \vec{p}) = -\lim_{\epsilon \to 0} \Gamma^{(2),E}(ip_0 \to -\omega - i\epsilon, \vec{p})$$

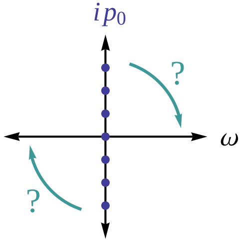

Spectral function is then given by

$$\rho(\omega, \vec{p}) = -\frac{1}{\pi} \mathrm{Im} \frac{1}{\Gamma^{(2),R}(\omega, \vec{p})}$$

[R.-A. T., N. Strodthoff, L. v. Smekal, and J. Wambach, Phys. Rev. **D 89**, 034010 (2014)]
[J. M. Pawlowski, N. Strodthoff, Phys. Rev. **D 92**, 094009 (2015)]
[N. Landsman and C. v. Weert, Physics Reports 145, 3&4 (1987) 141]

III) Results

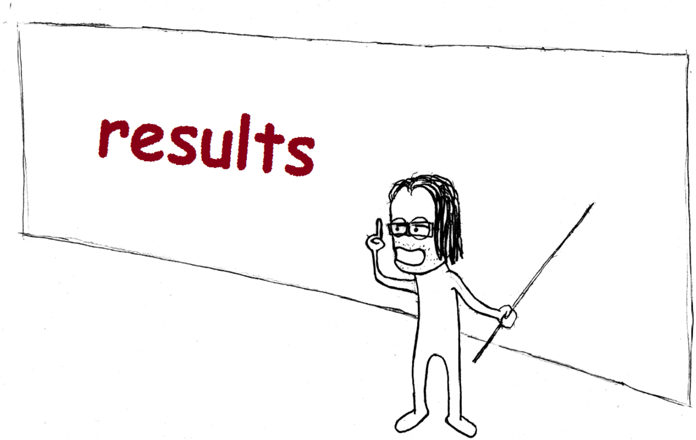

[courtesy L. Holicki]

Phase diagram of the quark-meson model

- chiral order parameter σ_0 decreases towards higher T and μ
- a crossover is observed at $T \approx 175$ MeV and $\mu = 0$
- critical endpoint (CEP) at $\mu \approx 292$ MeV and $T \approx 10$ MeV
- we will study spectral functions along $\mu = 0$ and $T \approx 10$ MeV

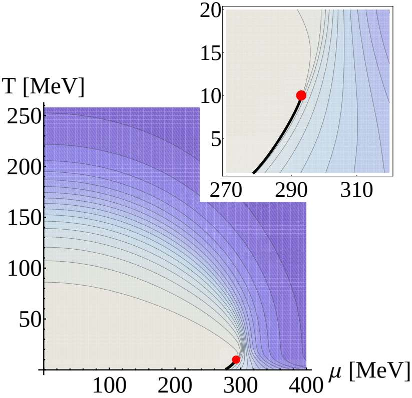

[R.-A. T., N. Strodthoff, L. v. Smekal, and J. Wambach, Phys. Rev. **D 89**, 034010 (2014)]

Phase diagram of the quark-meson model

- chiral order parameter σ_0 decreases towards higher T and μ
- a crossover is observed at $T \approx 175$ MeV and $\mu = 0$
- critical endpoint (CEP) at $\mu \approx 292$ MeV and $T \approx 10$ MeV
- we will study spectral functions along $\mu = 0$ and $T \approx 10$ MeV

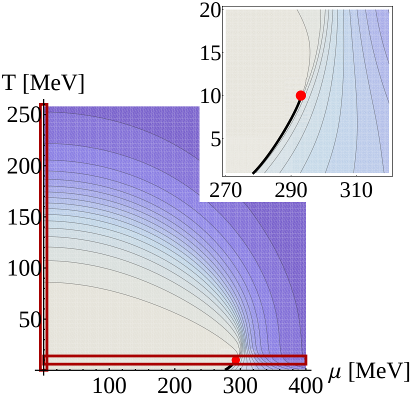

[R.-A. T., N. Strodthoff, L. v. Smekal, and J. Wambach, Phys. Rev. **D 89**, 034010 (2014)]

Flow of quark spectral function at $\mu = T = 0$

(Loading movie...)

Quark spectral function at $\mu = T = 0$

$\rho_{k,\psi}(\omega) = \gamma_0 \rho^{(C)}_{k,\psi}(\omega) + \rho^{(B)}_{k,\psi}(\omega)$

$\rho^{\pm}_k(\omega) = \mp \frac{1}{\pi} \mathrm{Im} G^{\pm}_k(\omega)$

$G^{\pm}_k(\omega) = \frac{1}{2} \mathrm{tr}\big(G_{k,\psi}(\omega)\Lambda_{\pm}\big)$

with $\Lambda_{\pm} = (1 \pm \gamma_0)/2$

$\int_{-\infty}^{\infty} d\omega\, \rho^{(C)}_{k,\psi}(\omega) = 1$

$\int_{-\infty}^{\infty} d\omega\, \rho^{(B)}_{k,\psi}(\omega) = 0$

$\rho^{(C)}_{k,\psi}(\omega) \geq |\rho^{(B)}_{k,\psi}(\omega)|$

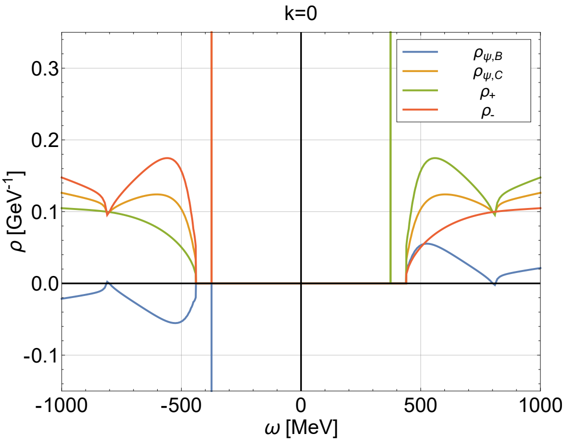

[R.-A. T., J. Weyrich, L. v. Smekal, and J. Wambach, arXiv:1807.11708]

Flow of σ and π spectral function at $\mu = T = 0$

(Loading movie...)

σ and π spectral function for $T > 0$ at $\mu = 0$

(Loading movie...)

σ and π spectral function for $\mu > 0$ at T_c

(Loading movie...)

σ spectral function vs. ω and $\vec{p}$ at $\mu = T = 0$

- time-like region ($\omega > \vec{p}$) is Lorentz-boosted to higher energies
- space-like region ($\omega < \vec{p}$) is non-zero at finite T due to space-like processes

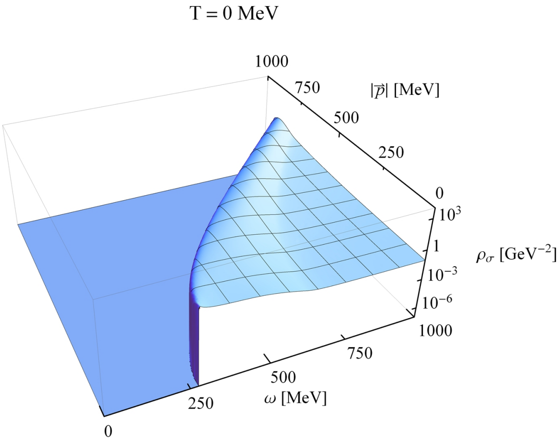

σ spectral function vs. ω and $\vec{p}$ for $T > 0$, $\mu = 0$

- time-like region ($\omega > \vec{p}$) is Lorentz-boosted to higher energies
- space-like region ($\omega < \vec{p}$) is non-zero at finite T due to space-like processes

(Loading movie...)

π spectral function vs. ω and $\vec{p}$ at $\mu = T = 0$

- time-like region ($\omega > \vec{p}$) is Lorentz-boosted to higher energies
- capture process $\pi^* + \pi \to \sigma$ is suppressed at large $\vec{p}$
- space-like region ($\omega < \vec{p}$) is non-zero at finite T due to space-like processes

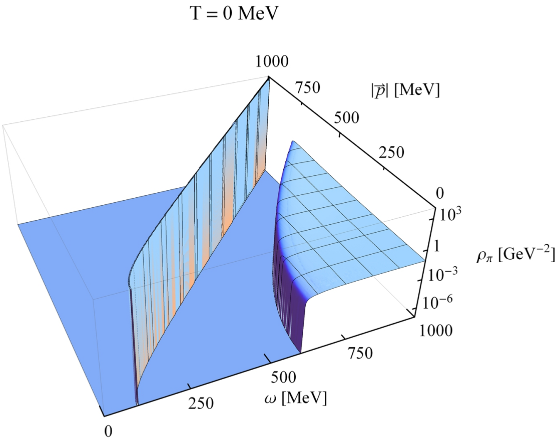

π spectral function vs. ω and $\vec{p}$ for $T > 0$, $\mu = 0$

- time-like region ($\omega > \vec{p}$) is Lorentz-boosted to higher energies
- capture process $\pi^* + \pi \to \sigma$ is suppressed at large $\vec{p}$
- space-like region ($\omega < \vec{p}$) is non-zero at finite T due to space-like processes

(Loading movie...)

Gauged linear-sigma model with quarks

- $SU(2)_L \times SU(2)_R$: corresponds to chiral symmetry of two-flavor QCD
- Additional gauge symmetry $U(1)$ to include photon field

Ansatz for the effective average action $\Gamma_k \equiv \Gamma_k[\sigma, \pi, \rho, a_1, \psi, \bar{\psi}, A_\mu]$:

$$\Gamma_k = \int d^4x \Big\{ \bar{\psi} \left(\not{D} - \mu\gamma_0 + h_S \left(\sigma + \mathrm{i}\vec{\tau}\vec{\pi}\gamma_5\right) + \mathrm{i}h_V \left(\gamma_\mu \vec{\tau}\vec{\rho}^{\mu} + \gamma_\mu\gamma_5\vec{\tau}\vec{a}_1^{\mu}\right)\right)\psi + U_k(\phi^2)$$

$$- c\sigma + \frac{1}{2}\left|(D_\mu - \mathrm{i}gV_\mu)\Phi\right|^2 + \frac{1}{8}\mathrm{Tr}\left(V_{\mu\nu}V^{\mu\nu}\right) + \frac{1}{4}m_{V,k}^2\mathrm{Tr}\left(V_\mu V^\mu\right) \Big\}$$

with

$$V_{\mu\nu} = D_\mu V_\nu - D_\nu V_\mu - \mathrm{i}g\left[V_\mu, V_\nu\right], \quad D_\mu\psi = \left(\partial_\mu - \mathrm{i}eA_\mu Q\right)\psi,$$

$$D_\mu V_\mu = \partial_\mu V_\nu - ieA_\mu[T_3, V_\nu], \quad \phi \equiv (\vec{\pi}, \sigma), \quad V_\mu \equiv \vec{\rho}_\mu\vec{T} + \vec{a}_{1,\mu}\vec{T}^5$$

Flow equations for ρ and a_1 2-point functions

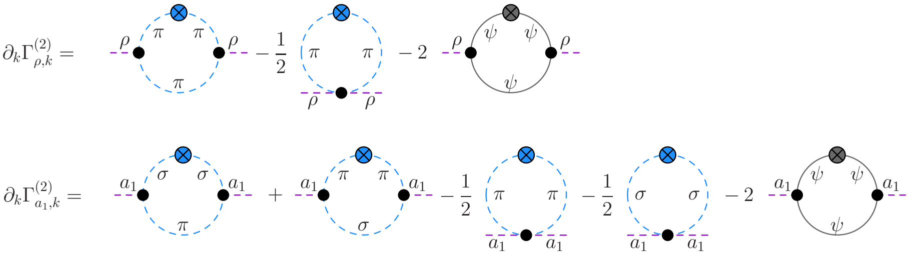

- neglect vector mesons inside the loops
- vertices extracted from ansatz for the effective average action Γ_k
- tadpole diagrams give ω-independent contributions

[C. Jung, F. Rennecke, R.-A. T., L. von Smekal, and J. Wambach, Phys. Rev. **D 95**, 036020 (2017)]

ρ and a_1 vacuum spectral functions

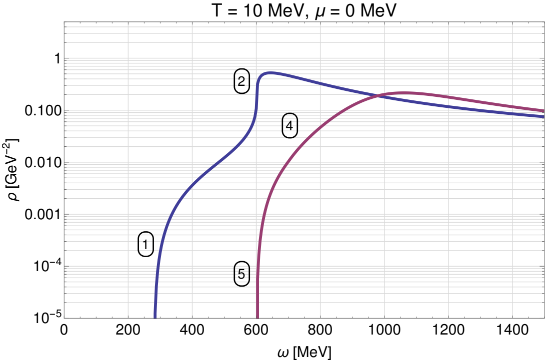

(1) : $\rho^* \to \pi + \pi$

(2) : $\rho^* \to \bar{\psi} + \psi$

(3) : $a_1^* + \pi \to \sigma$

(4) : $a_1^* \to \pi + \sigma$

(5) : $a_1^* \to \bar{\psi} + \psi$

[C. Jung, F. Rennecke, R.-A. T., L. von Smekal, and J. Wambach, Phys. Rev. **D 95**, 036020 (2017)]

T-dependence of ρ and a_1 spectral functions

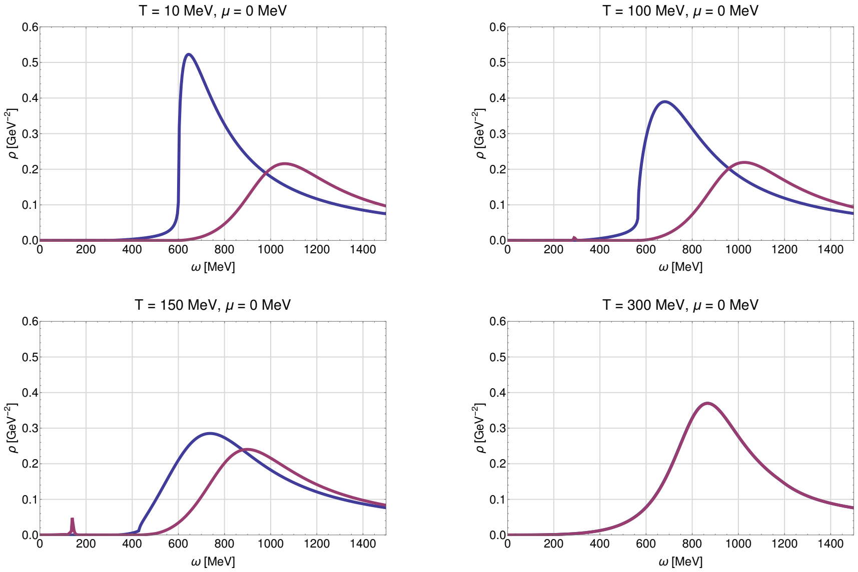

[C. Jung, F. Rennecke, R.-A. T., L. von Smekal, and J. Wambach, Phys. Rev. **D 95**, 036020 (2017)]

μ-dependence of ρ and a_1 spectral functions

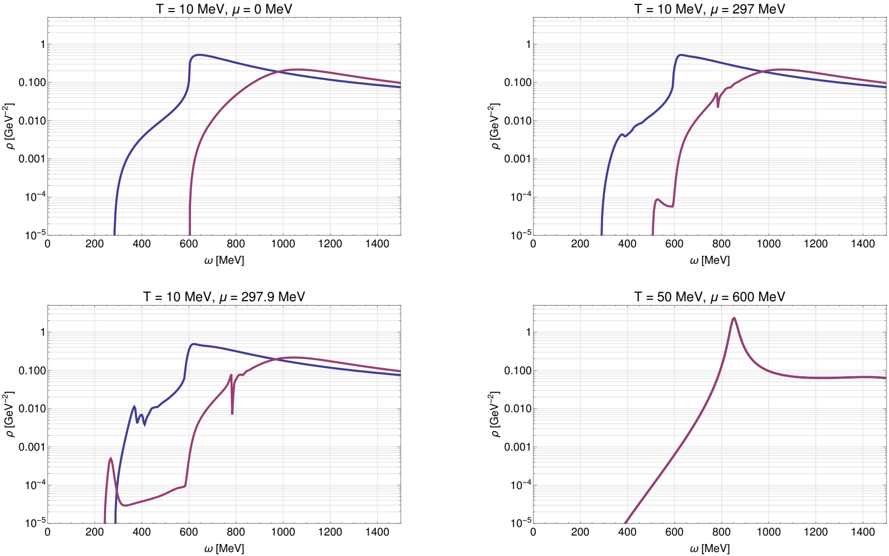

[C. Jung, F. Rennecke, R.-A. T., L. von Smekal, and J. Wambach, Phys. Rev. **D 95**, 036020 (2017)]

T-dependence of ρ and a_1 spectral functions

(Loading movie...)

T-dependence of ρ and a_1 pole masses

- pole masses in the vacuum:

$$m_\rho^p = 789 \text{ MeV}, \quad m_{a_1}^p = 1275 \text{ MeV}$$

- degeneration of ρ and a_1 spectral functions in chirally symmetric phase
- broadening of spectral functions with increasing T
- pole masses do not vary much, no dropping ρ mass

$\Rightarrow$ consistent with broadening/melting-ρ-scenario

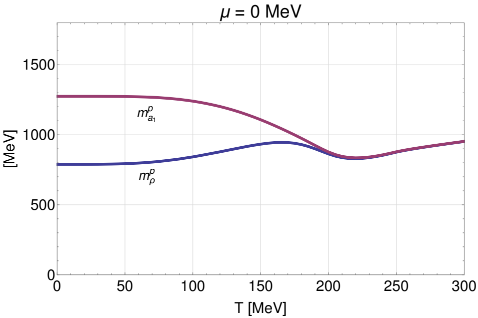

[C. Jung, F. Rennecke, R.-A. T., L. von Smekal, and J. Wambach, Phys. Rev. **D 95**, 036020 (2017)]

Momentum-dependence of ρ spectral function

- shown for $\mu = 0$ and $T = 100$ MeV
- time-like region ($\omega > \vec{p}$) is Lorentz-boosted to higher energies
- space-like region ($\omega < \vec{p}$) is non-zero at finite T due to space-like processes

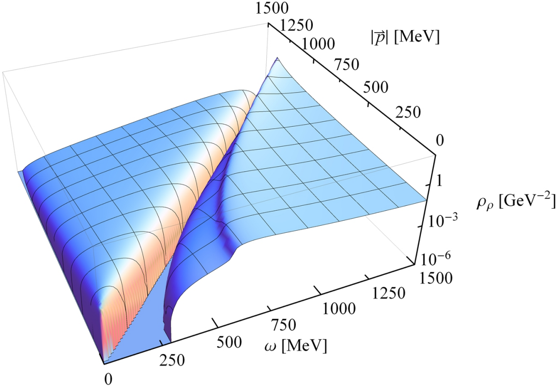

[C. Jung, F. Rennecke, R.-A. T., L. von Smekal, and J. Wambach, Phys. Rev. **D 95**, 036020 (2017)]

Temperature-dependence of ρ spectral function

- time-like region ($\omega > \vec{p}$) is Lorentz-boosted to higher energies
- space-like region ($\omega < \vec{p}$) is non-zero at finite T due to space-like processes

(Loading movie...)

[C. Jung, F. Rennecke, R.-A. T., L. von Smekal, and J. Wambach, Phys. Rev. **D 95**, 036020 (2017)]

Electromagnetic (EM) spectral function

$$\begin{pmatrix} \Gamma^{(2)}_{AA} & \Gamma^{(2)}_{A\rho} \\ \Gamma^{(2)}_{\rho A} & \Gamma^{(2)}_{\rho\rho} \end{pmatrix} \xrightarrow{\text{diagonalize}} \begin{pmatrix} \tilde{\Gamma}^{(2)}_{AA} & 0 \\ 0 & \tilde{\Gamma}^{(2)}_{\rho\rho} \end{pmatrix}, \quad \tilde{\Gamma}^{(2)}_{AA} = \overbrace{\Gamma^{(2)}_{AA} - \frac{\Gamma^{(2)}_{A\rho}\Gamma^{(2)}_{\rho A}}{\Gamma^{(2)}_{\rho\rho}}}^{\mathcal{O}(e^2)} + \mathcal{O}(e^4)$$

$\partial_k \Gamma^{(2)}_{\rho\rho,k} =$

$\partial_k \Gamma^{(2)}_{AA,k} =$

$\partial_k \Gamma^{(2)}_{A\rho,k} =$

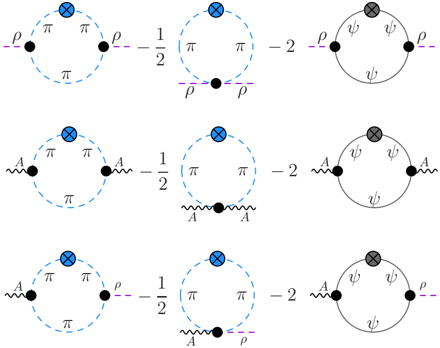

[R.-A. T., C. Jung, N. Tanji, L. von Smekal, and J. Wambach, arXiv:1807.04952]

EM spectral function - preliminary

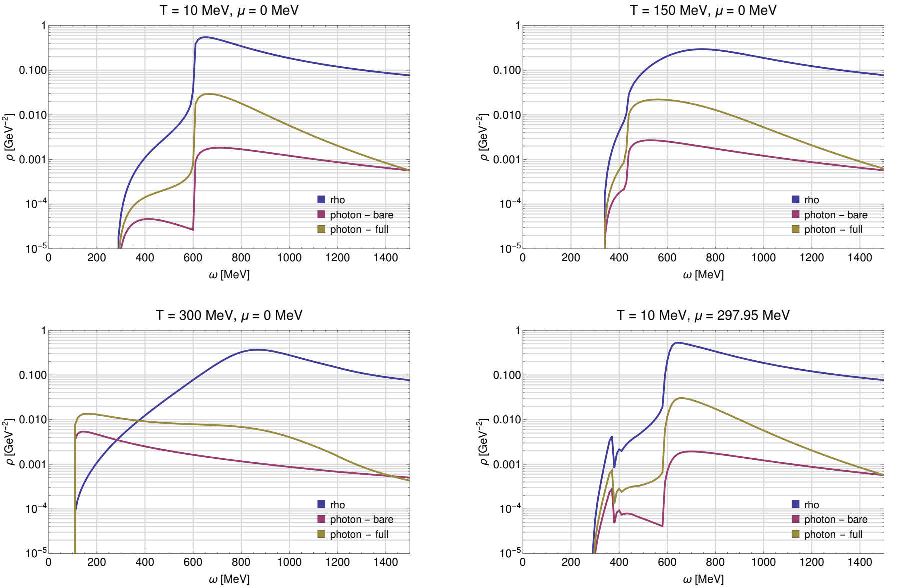

[R.-A. T., C. Jung, N. Tanji, L. von Smekal, and J. Wambach, arXiv:1807.04952]

Calculation of dilepton rates

- We use the Weldon formula for the thermal dilepton rate:

$$\frac{d^8 N_{l\bar{l}}}{d^4 x d^4 q} = \frac{\alpha}{12\pi^3}\left(1+\frac{2m^2}{q^2}\right)\left(1-\frac{4m^2}{q^2}\right)^{1/2} q^2 (2\rho_T + \rho_L) n_B(q_0)$$

- in the following we assume $m = 0$ and set the external spatial momentum to zero, such that $\rho_T = \rho_L = \rho_{\tilde{A}\tilde{A}}$

[H. A. Weldon, Phys. Rev. D42, 2384 (1990)]

[R.-A. T., C. Jung, N. Tanji, L. von Smekal, and J. Wambach, arXiv:1807.04952]

Dilepton rates - preliminary

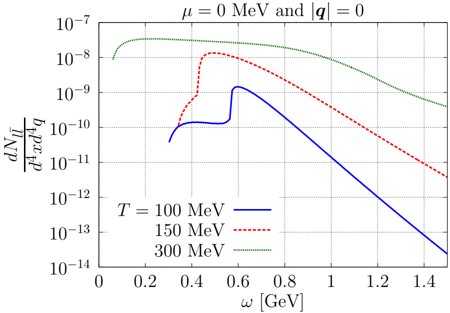

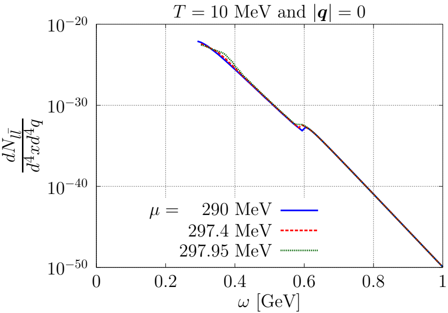

- clear changes are visible with increasing temperature
- no distinct signatures for the critical endpoint yet $\rightarrow$ improve truncation

[R.-A. T., C. Jung, N. Tanji, L. von Smekal, and J. Wambach, arXiv:1807.04952]

Summary and Outlook

- analytically continued flow equations for quark and (vector-)meson spectral functions using effective models for QCD within a consistent FRG framework
- degeneracy of ‘parity partners’ due to restoration of broken chiral symmetry in the QCD medium

Outlook:

- study the quark spectral function at finite density and temperature
- improve truncation (include baryons and more decay channels) to calculate realistic dilepton rates and identify signatures of phase transitions
- calculate transport coefficients like the shear viscosity and the electrical conductivity